

# An Activable Nanoscintillator Probe for Detecting Telomerase Activity and Screening Inhibitors In Vivo

Baoliu Chen,<sup>1</sup> Junduan Dai,<sup>1</sup> Sijie Song,<sup>1</sup> Xianzhe Tang,<sup>1</sup> Yuheng Guo,<sup>1</sup> Ting Wu,<sup>1</sup> Mengnan Wu,<sup>1</sup> Chaojie Hao,<sup>1</sup> Xiaofeng Cheng,<sup>1</sup> Xucong Lin,<sup>2</sup> Yijie Bian,<sup>3,\*</sup> Zhaowei Chen,<sup>1,\*</sup> and Huanghao Yang<sup>1,\*</sup>

<sup>1</sup>MOE Key Laboratory for Analytical Science of Food Safety and Biology, New Cornerstone Science Laboratory, Fujian Provincial Key Laboratory of Analysis and Detection Technology for Food Safety, and State Key Laboratory of Photocatalysis on Energy and Environment, College of Chemistry, Fuzhou University, Fuzhou 350108, P. R. China.

<sup>2</sup>Engineering Technology Research Center on Reagent and Instrument for Rapid Detection of Product Quality and Food Safety in Fujian Province, College of Chemistry, Fuzhou University, Fuzhou 350108, China.

<sup>3</sup>College of Biological Science and Engineering, Fuzhou University, Fuzhou 350108, P. R. China.

\* Correspondence: bianyijie@fzu.edu.cn; chenzw@fzu.edu.cn; hhyang@fzu.edu.cn

## Additional information on reagents and materials, characterizations, experimental details, DNA sequences, and cell culture, etc.

**Reagents and materials.** Deionized ultrapure water (18.2 MΩ·cm<sup>-1</sup>; Millipore CO., USA) was used in all experiments. Lanthanide acetate (Ln(CH<sub>3</sub>COO)<sub>3</sub>·4H<sub>2</sub>O) (Ln= Lu, Gd, Tb, Y), sodium hydroxide, oleic acid, ammonium fluoride, 1-octadecene, tetraethyl orthosilicate, 1-methylethanol, 3-aminopropyltriethoxysilane, *N*-hydroxysuccinimide, succinic anhydride, *N*-(3-(dimethylamino)propyl)-*N*-ethylcarbodiimide, trypsin, glutathione, thrombin, trypsin, lysozyme, glucose, 3-[(3-cholamidopropyl)dimethylammonio]-1-propanesulfonic acid (CHAPS), 3'-azido-3'-deoxythymidine, curcumin, doxorubicin, cisplatin, epigallocatechin gallate and 2-[(*E*)-3-naphthalen-2-ylbut-2-enoylamino]benzoic acid were purchased from Sigma-Aldrich (Shanghai, China). All chemicals were analytical grade and used without further purification unless otherwise stated. Deoxynucleotide solution mixture was purchased from New England Biolabs (Beijing, China). Cell Counting Kit-8 (CCK-8) was purchased from Beyotime (Shanghai, China). Dulbecco's modified Eagle's medium, RPMI-1640 medium, fetal bovine serum, and penicillin/streptomycin were obtained from Life Technologies (Carlsbad, CA). All HPLC-purified oligonucleotides (see Table S1) were purchased from Sangon Biotechnology Co., Ltd. (Shanghai, China).

**Characterization.** Transmission electron microscopy (TEM) was taken on a Tecnain G2 F20 S-TWIN microscope (200 kV, FEI Nano Ports, USA). X-ray induced fluorescence measurements were performed using an Edinburgh FS5 fluorescence spectrophotometer (Edinburgh Instruments Ltd., UK) at an X-ray dose rate of 278 μGy/s at a voltage of 50 kV and a current of 80 μA. The X-ray photons were generated from a mini-X-ray tube (Amptek, Inc., USA). Zeta potential and hydrated particle size were measured by a Zetasizer Nano particle analyzer (Malvern Instruments Ltd., England). Fourier transform infrared spectra (FTIR) were obtained by a Nicolet 6700 spectrometer (Thermo Scientific, Madison, USA). Ultraviolet-visible-near-infrared light (UV-vis-NIR) absorption spectra were measured by a UH4150 Spectrophotometer (Hitachi Co. Ltd., Japan). The CCK-8 results were measured in a microplate reader (Infinite 200 PRO, Tecan). The images of gel electrophoresis were captured by a ChemiDOCTM Touch Imaging System (Bio-Rad, USA). Confocal microscopy assay was operated on a laser-scanning confocal microscopy system (NIKON, A1, Japan). X-ray induced fluorescence imaging was performed on a small animal imaging system (Spectral Instruments Imaging Co., USA) at an X-ray dose of 278 μGy/s with 30 s exposure.

**Quantitation of the content of BHQ1 in the probe.** The quantification of DNA device is calculated according to the amount of BHQ1 in the probe, as only DNA devices containing BHQ1 molecules can simultaneously quench the luminescence of

nanoscintillators and respond to telomerase. To measure the content of BHQ1 in the probe, a series of BHQ1-strand solutions was prepared and obtained a standard curve with recording the absorption intensity in 546 nm (Figure S5) by microplate reader. Then the absorbance intensity at 546 nm in the probe was 0.1194, the amount of BHQ1-strand in the probe was estimated to be around 0.4966 nmol, corresponding to 0.4966 nmol BHQ1-strand per mg probe.

**Cell culture.** All cell lines were obtained from American Type Culture Collection (ATCC, Manassas, VA). HeLa (human cervical cancer cell line), HepG2 cells (human hepatocellular carcinoma cells), A549 cells (human lung cancer cells), and Caco-2 cells (human colon cancer cells) were cultured in Dulbecco's modified Eagle's medium (DMEM, Gibco). MCF-7 (human lung cancer cell line), L02 cells (the normal human liver cell line) were cultured in medium of RPMI-1640 (Gibco). The cell growth media were supplemented with 10% fetal bovine serum (FBS, Gibco) and 1% penicillin-streptomycin and cultured at 37 °C in a 5% CO<sub>2</sub> humidified environment.

**Gel electrophoresis.** 1 μL of TP, 1 μL of BHQ1-strand and 1 μL of A-strand were added to 15 μL of 1× TRAP reaction buffer (20 mM Tris-HCl, pH 8.3, 63 mM KCl, 1.5 mM MgCl<sub>2</sub>, 0.005% Tween 20 and 0.2 mM EGTA) in a centrifuge tube, and the mixture was incubated at 33 °C for 3 h to form the hybridized-DNA, after the reaction was end, 50 μL of cell lysate solution and 50 μL dNTP (200 μM) were added to the hybridized-DNA solution and the resultant solution was incubated at 37 °C for 2 h to extend the telomerase primer. For gel electrophoresis, the resultant solution of each group was mixed with 2.0 μL of loading buffer and loaded onto polyacrylamide hydrogel. Electrophoresis was carried out in tris-borate-EDTA (TBE) buffer at 120 V for 120 min. The gel was stained for 10 min with 4S Red Plus and imaged using with a Tocan 240 gel imaging system (Shanghai Tocan Biotechnology Company).

**Cytotoxicity assay.** The cytotoxicity of the probe was assessed by a CKK-8 method. HeLa and L02 cells were seeded in a 96-well plate with density of 10,000 cells/well at 37 °C for 24 h, followed by replacing the culture medium with fresh cell culture media containing various concentrations of the probe (0, 20, 40, 60, 100, 150, and 200 μg/mL). The cells were further incubated at 37 °C for another 24 h, and then the cells were washed with PBS and replaced with fresh medium contained CKK-8 solution (200 μl) and incubated for 1 h. Afterwards, the absorption in each well at 450 nm were recorded by a microplate reader. The cell viability values were calculated by the formula:  $([Abs]_{test}/[Abs]_{control}) \times 100\%$ , where  $[Abs]_{test}$  and  $[Abs]_{control}$  were the absorption values at 450 nm of treated cells (20, 40, 60, 100, 150, and 200 μg/mL) and nontreated cells (0 μg/mL), respectively.

**Cellular uptake of the Probe.** HeLa and L02 cells ( $1 \times 10^5$ ) were seeded in 35 mm glass-bottom confocal dishes and incubated at 37 °C overnight. After removing the culture medium and washed with PBS buffer, 1 mL of fresh medium containing the Cy3-labeled probe (25 μg/mL) was added and the cells were incubated for different times (0, 1, 2, 3, and 4 h). After removing the free probe with PBS, the nuclei were stained with Hoechst 33342 for another 10 minutes at 37 °C. Then, the fluorescent images were acquired on a Nikon SIM confocal laser scanning microscope. Cy3 was excited at 510-560 nm and detected with a BA 570-650 nm barrier filter.

**Biosafety analysis.** To test the biosafety of the probe, healthy mice were intravenously injected with 50 μL of the probe (5 mg/mL) in saline. Mice injected with the same volume of saline were set as the control group. Following that, the mice were weighed every other 2 days from 0 to 20 days. Meanwhile, at day 10 and 20 post injection, blood samples were collected for blood biochemistry test. Also, at day 20, the major organs of the mice (heart, liver, spleen, lung, and kidney) were harvested and fixed using 4% paraformaldehyde for Hematoxylin and eosin (H&E) staining analysis.

**Tissue penetration depth of X-ray.** To study the tissue penetration depth of X-ray, capillaries were filled with probes pretreated with telomerase extracts from HeLa cells. Afterwards, the X-ray induced fluorescence imaging of the capillaries with pork of different thickness (1.0, 1.5, 2.0 and 2.5 cm) placed between the X-ray light sources and the capillaries were acquired.

**Autofluorescence assay.** To study autofluorescence generated in vitro,  $1 \times 10^5$  HeLa cell suspensions were excited by X-ray or UV light (365 nm) and the fluorescence spectrum was recorded correspondingly. Also, the sample solution in tube was imaged under the X-ray or UV excitation. To study autofluorescence generated in vivo, HeLa tumour-bearing mice were imaged upon excitation by X-ray or UV light (365 nm).

### Supporting Figures

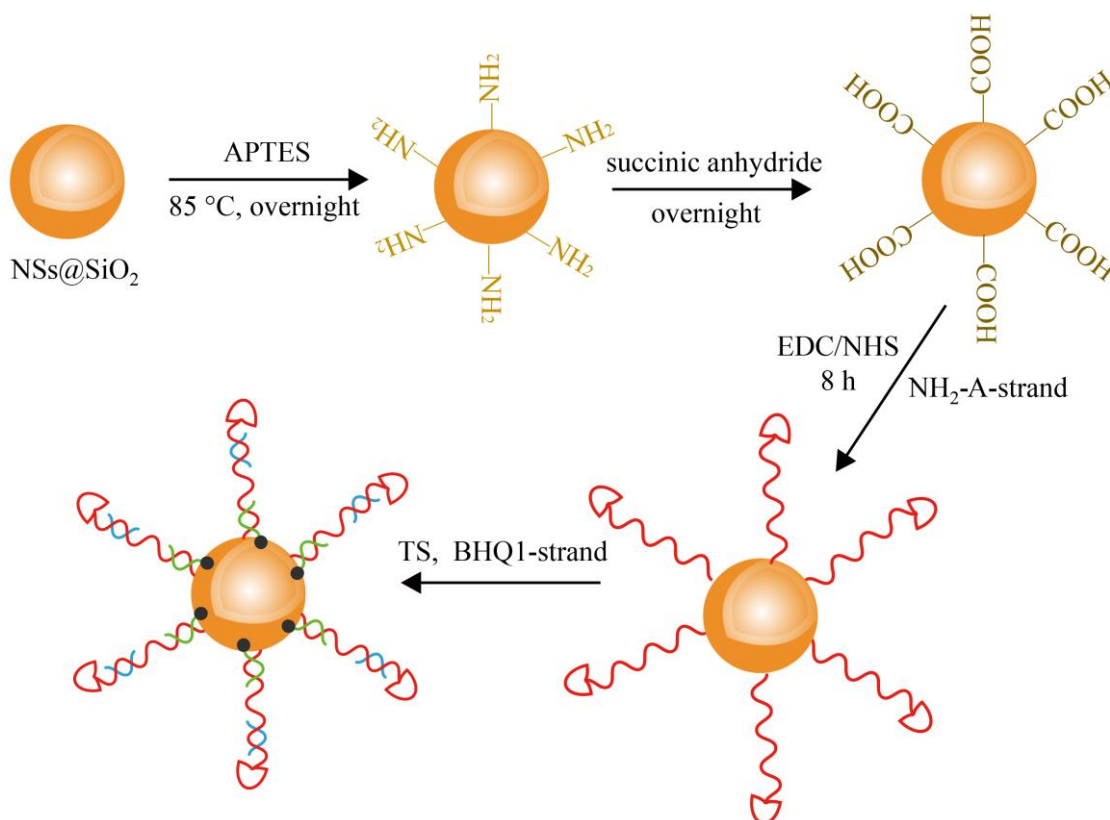


**Figure S1.** Schematic illustration of the synthetic process of the probe.

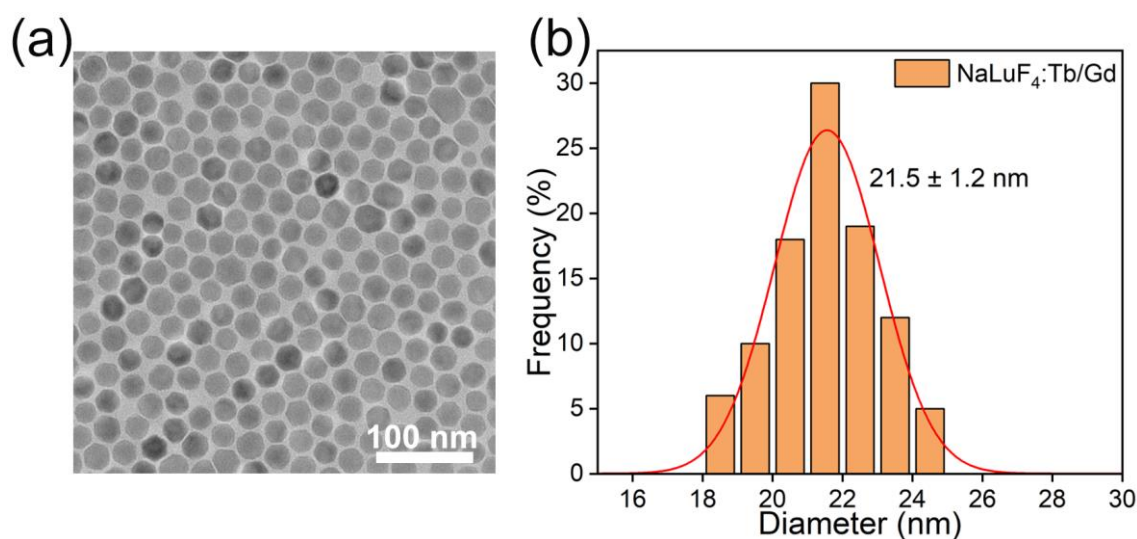


**Figure S2.** Synthesis and characterization of NaLuF<sub>4</sub>:Tb/Gd nanoparticles. (a) Transmission electron microscopy (TEM) image of NaLuF<sub>4</sub>:Tb/Gd. The obtained nanoparticles manifested a hexagonal morphology and had a good dispersibility. Scale bar, 100 nm. (b) Size distribution of NaLuF<sub>4</sub>:Tb/Gd nanoparticles, which was analyzed from a.

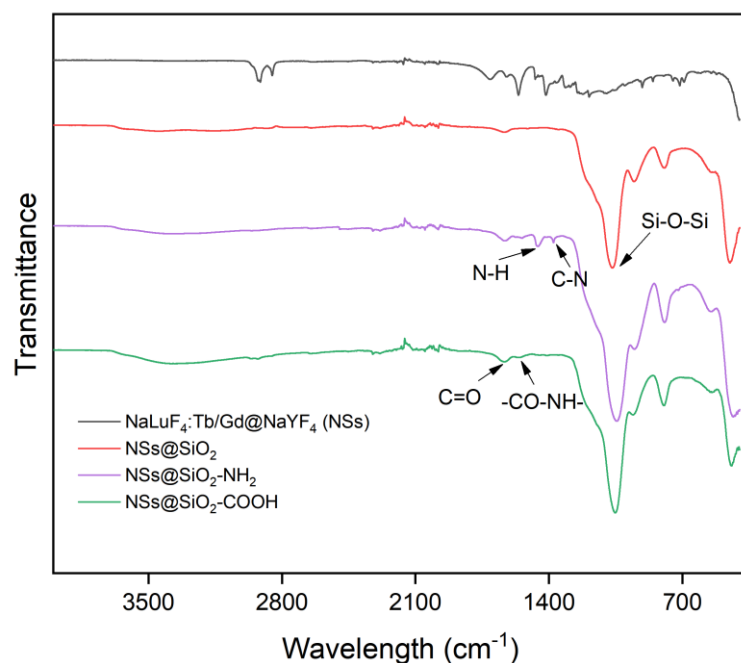


**Figure S3.** FTIR spectra of the oleate capped NaLuF<sub>4</sub>:Tb/Gd@NaYF<sub>4</sub> (NSs), NSs@SiO<sub>2</sub>, NSs@SiO<sub>2</sub>-NH<sub>2</sub>, and NSs@SiO<sub>2</sub>-COOH particles.

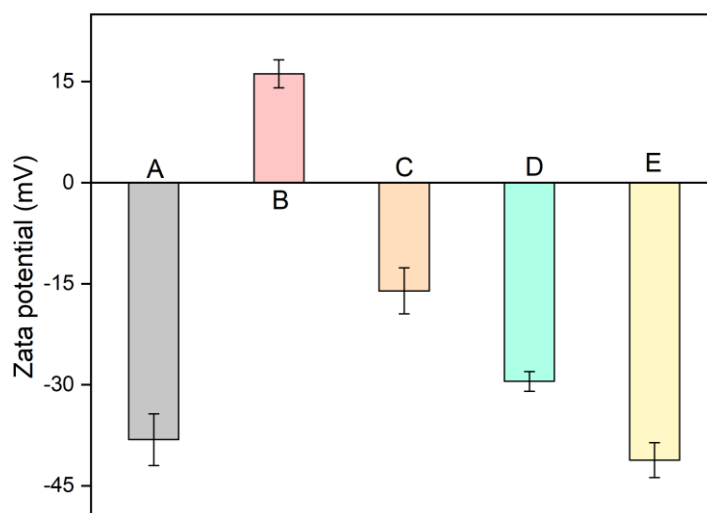


**Figure S4.** Zeta potential of NSs@SiO<sub>2</sub> particles (A), NSs@SiO<sub>2</sub>-NH<sub>2</sub> particles (B), NSs@SiO<sub>2</sub>-COOH particles (C), NSs@SiO<sub>2</sub>-A-strand particles (D), and probe (E). There was an increase in zeta potential from -38.14 mV to 16.16 mV after amino functionalized NSs@SiO<sub>2</sub> particles; the zeta potential decreased to -16.05 mV after grafting of the carboxyl groups, and further decreased from -29.49 mV to -41.18 mV after hybridizing the A-strand with the telomerase primer sequence and the BHQ1-strand. Error bars represented the standard deviations of three independent experiments.

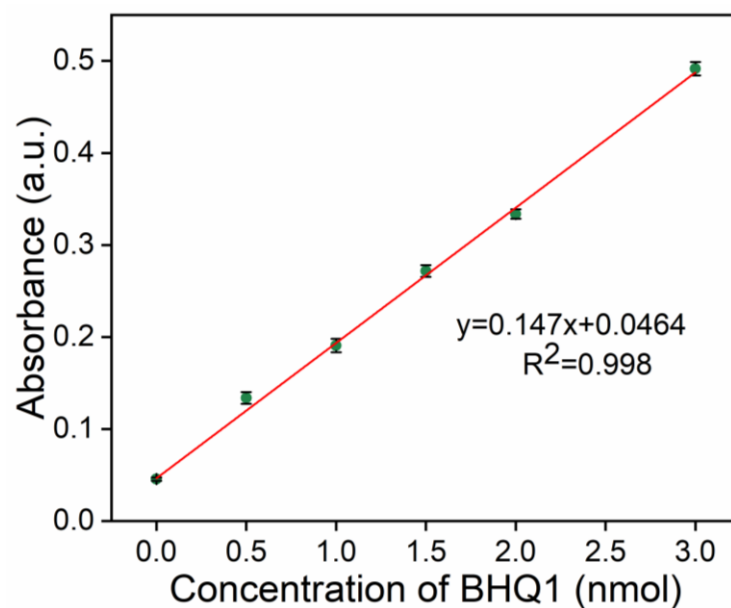


**Figure S5.** Plot of the absorbance of BHQ1-strand at 546 nm versus the concentration of BHQ1-strand. Error bars represented the standard deviation of three independent experiments.

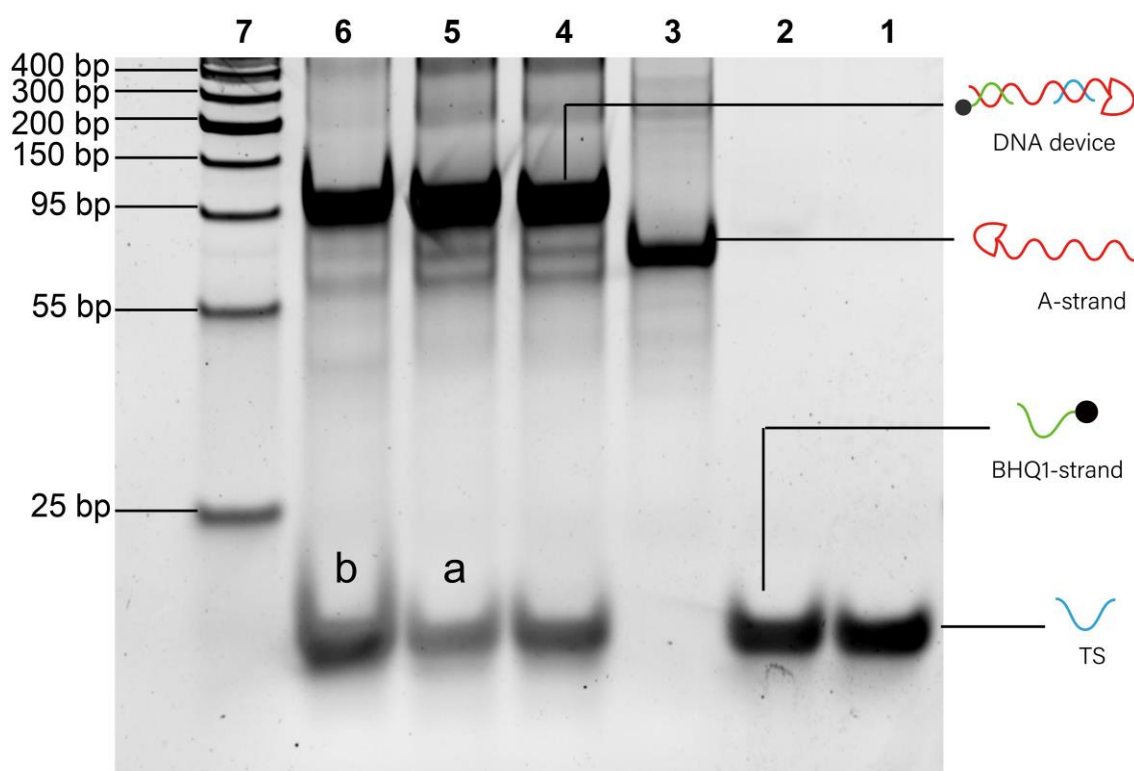


**Figure S6.** Gel electrophoresis of the telomerase-responsive DNA devices (DMDs) and the telomerase-triggered telomerase primer extension and strand displacement. lane 1: telomerase primer (TP); lane 2: BHQ1-strand; lane 3: A-strand; lane 4: telomerase-responsive DNA devices (DMDs); lane 5: DMDs and dNTP incubated in 37 °C for 2 h; lane 6: DMDs, dNTP and telomerase extract incubated at 37 °C for 2 h; Lane 7: DNA marker. The lane 4 presented a gel band of approximately 99 bp which was the same as the total bases of the three sequences (lanes 1, 2, and 3), implying the formation of the DMDs. In lane 5, without telomerase, no replacement and release of BHQ1-strand was observed. However, upon addition of telomerase to the solution containing DMDs and dNTPs, a stronger band (6-b) corresponding to BHQ1-strand were observed in lane 6 compared to the similar position in lane 5 (band 5-a). These results implied that telomerase extended the telomerase primer and led to the release of the BHQ1-strand by strand displacement reaction.

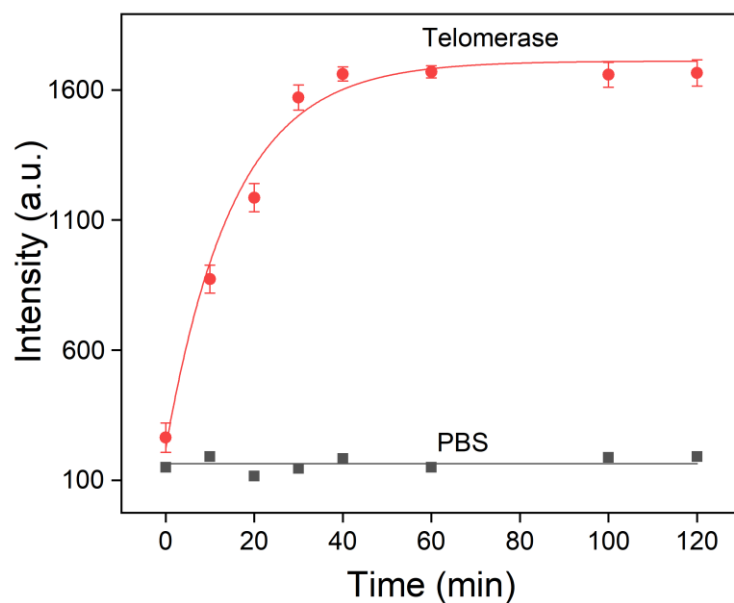


**Figure S7.** Fluorescence changes at 546 nm of the probe after incubated with telomerase extracts and PBS for different reaction time. Fluorescence signal increased after the addition of telomerase extracts from  $1 \times 10^5$  HeLa cells over time. Probes treated with PBS was set as a control. Error bars represented the standard deviation of three independent experiments.

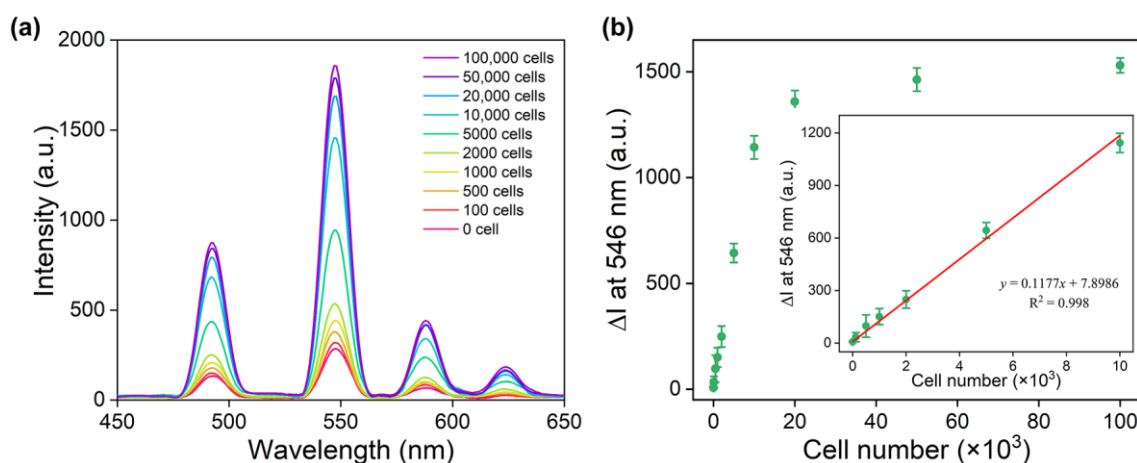


**Figure S8.** (a) X-ray induced fluorescence spectra of the probe after incubation with telomerase extracts from different numbers of HepG2 cells. (b) The relationship between fluorescence intensity enhancement ( $\Delta I$ ) at 546 nm and HepG2 cell numbers. Inset: linear plot of the fluorescence enhancement versus HepG2 cell numbers. Error bars represented the standard deviation of three independent experiments.

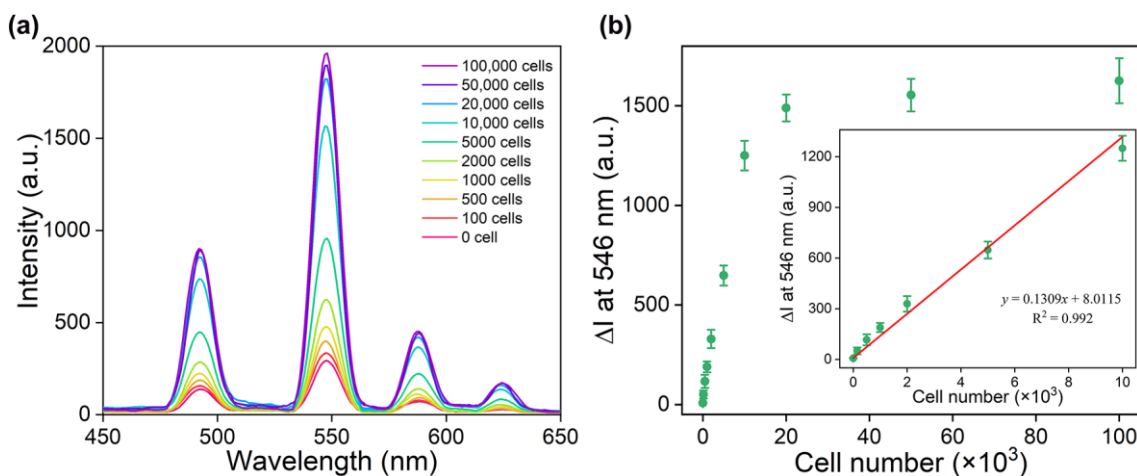


**Figure S9.** (a) X-ray induced fluorescence spectra of the probe after incubation with telomerase extract from different numbers of MCF-7 cells. (b) The relationship between fluorescence intensity enhancement ( $\Delta I$ ) at 546 nm and MCF-7 numbers. Inset: linear plot of the fluorescence enhancement versus MCF-7 cell numbers. Error bars represented the standard deviation of three independent experiments.

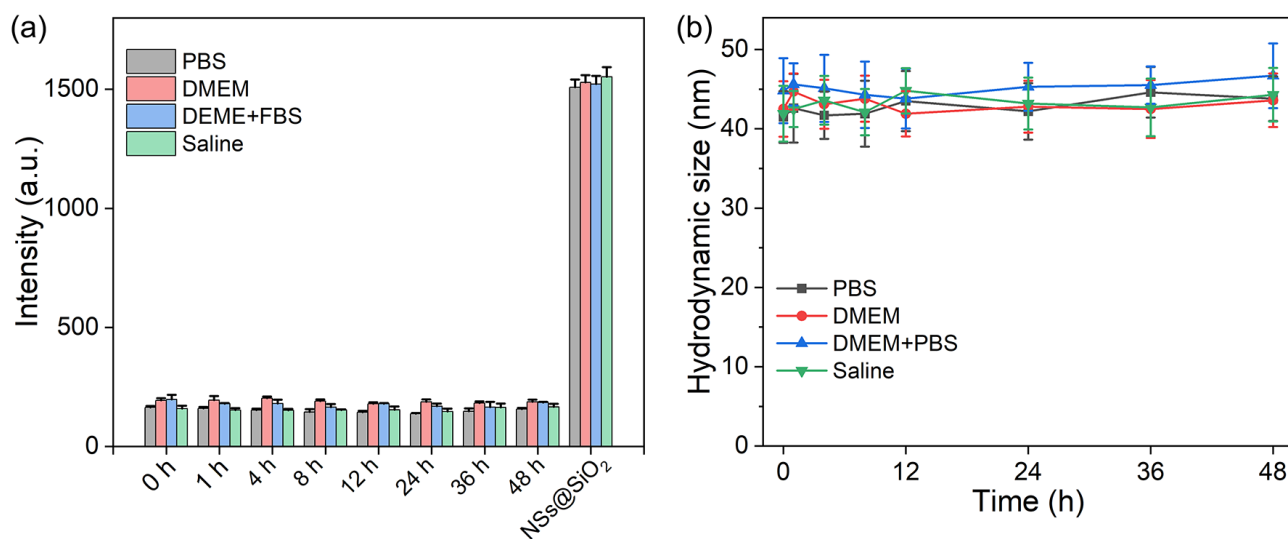


**Figure S10.** The stability of the probe in different solutions after incubation at 37 °C for different time. (a) The X-ray induced fluorescence intensity at 546 nm of the probe changed negligibly even after incubation for 48 h, implying that the probe had good stability against nonspecific activation. NSs@SiO<sub>2</sub> particles in these solutions was set as the control. (b) The average hydrodynamic size of the probe showed insignificant changes after incubation in different solutions as indicated for different time, showcasing the colloidal stability of the probe. Error bars represented the standard deviations of three independent experiments.

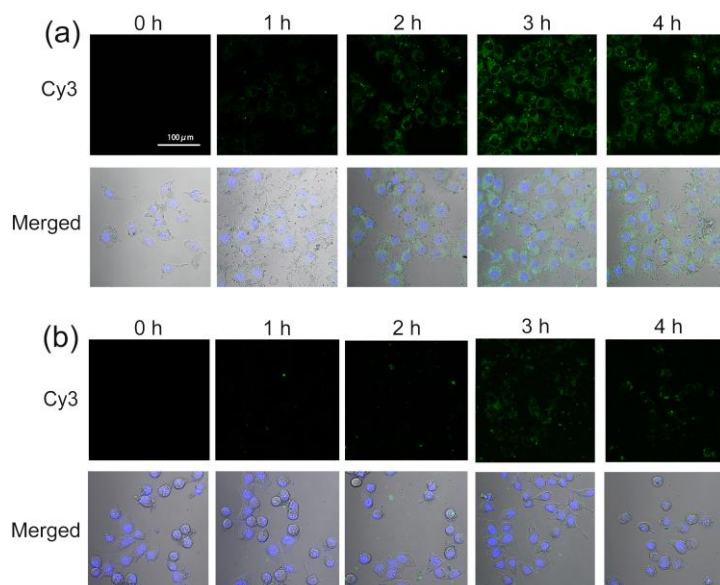


**Figure S11.** Confocal laser scanning microscopy (CLSM) fluorescence images of (a) HeLa cell and (b) L02 cells after treated with the probe for 0, 1, 2, 3, and 4 h. The BHQ1-strand was replaced by Cy3 (green)-labeled strand for direct visualization under CLSM. The nuclei were stained with DAPI (blue). All images share the same scale bar.

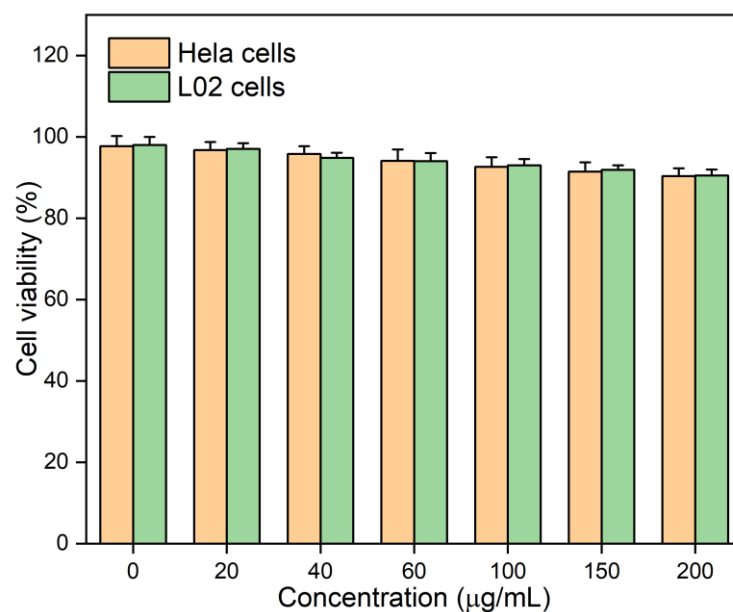


**Figure S12.** Cell viabilities of HeLa and L02 cells after treated with different concentrations of probe for 24 h. The results showed that the probe exhibited a satisfactorily low cytotoxicity even at concentration of 200 µg/mL. Error bars represented the standard deviations of three independent experiments.

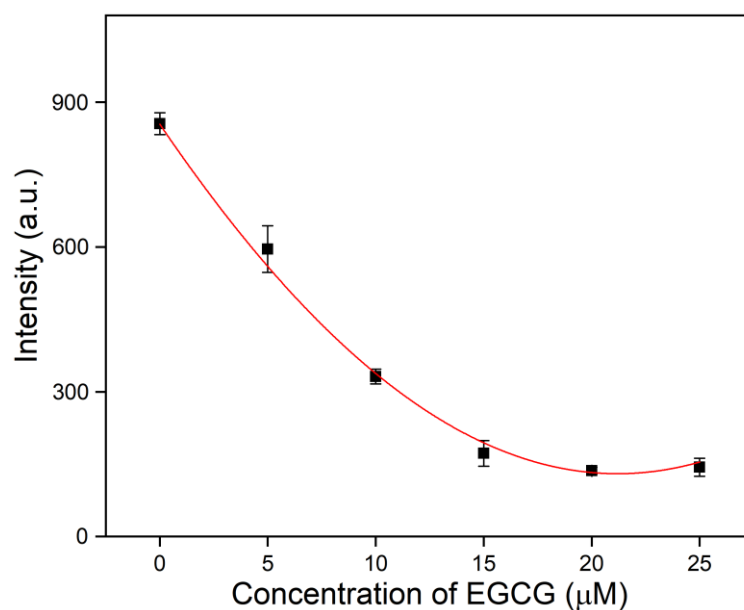


**Figure S13.** Inhibition of telomerase activity by EGCG. The X-ray induced fluorescence signal at 546 nm of the probe gradually declined upon increasing the concentration of EGCG and reached a plateau over 20 µM, the result indicated that the probe could read out the dose-dependent inhibition of EGCG toward telomerase activity. Error bars represented the standard deviation of three independent experiments.

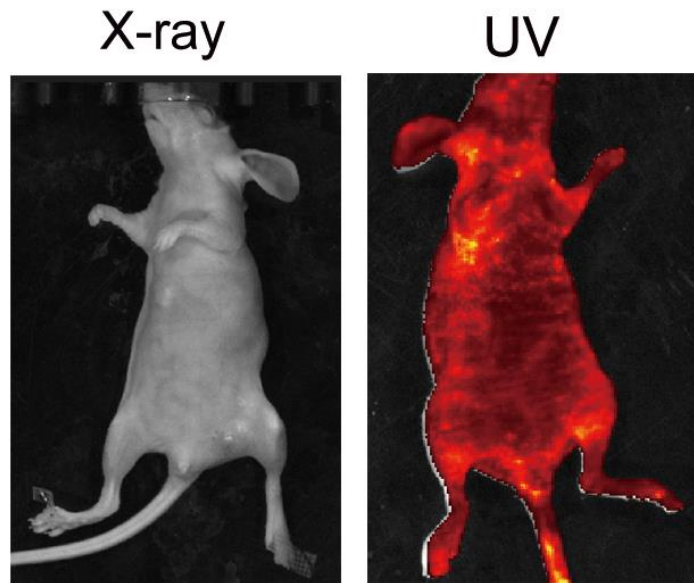


**Figure S14.** Comparison of the autofluorescence background under excitations of UV (365 nm) and X-ray source. Fluorescence imaging of nude mice under the excitation of X-ray (left) and UV (right) light. The results showed there was no autofluorescence under X-ray excitation compared to that under the UV excitation.

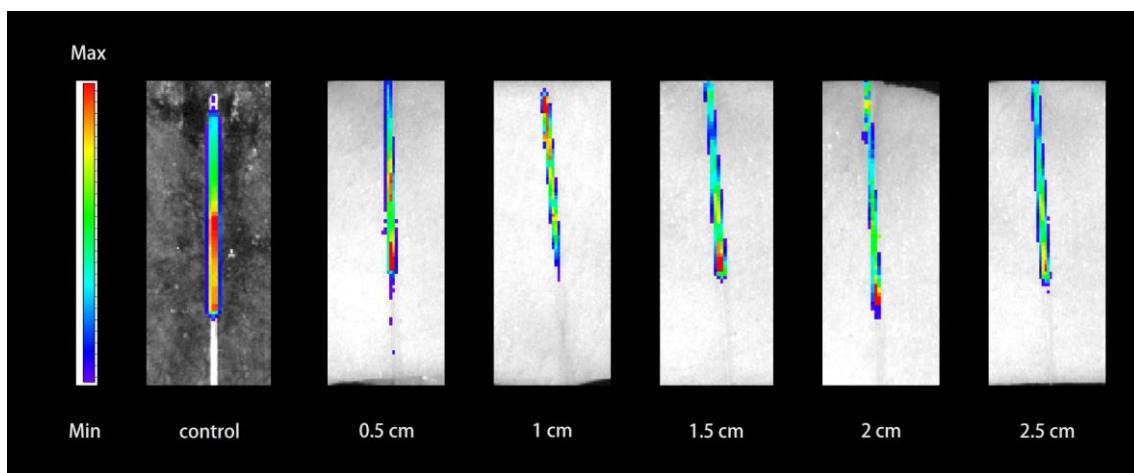


**Figure S15.** Evaluation of the tissue penetration depth of X-ray. The experiment was performed by placing pork slices of different thickness between the X-ray source and telomerase-activated probe. The results showed that the X-ray induced fluorescence of the telomerase-activated probe was clearly presented under X-ray activation even when the thickness of the pork was up to 2.5 cm, validating that X-ray had deep tissue penetration capacity.

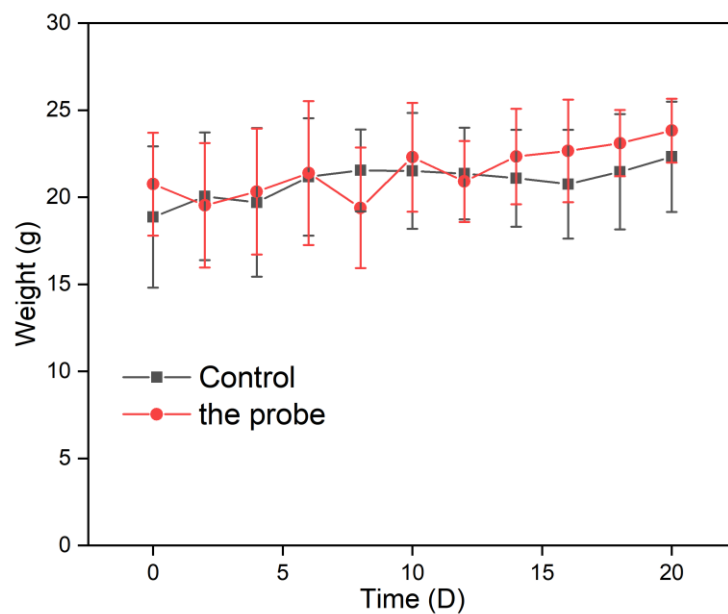


**Figure S16.** Body weight changes of healthy mice after intravenous injection of the probe and saline for different time. The saline group was used as the control. Error bars represented the standard deviation of five mice.

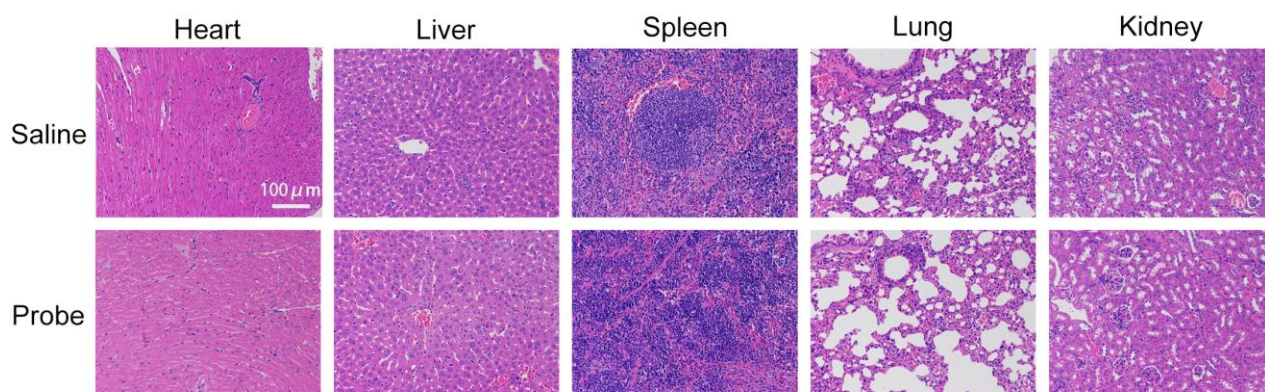


**Figure S17.** H&E-stained tissue sections of the major organs (heart, liver, spleen, lung, and kidney) after intravenous injection of the probe and 0.9 % saline for 20 days. No obvious signs of pathological damage were observed, indicating the biocompatibility of the probe.

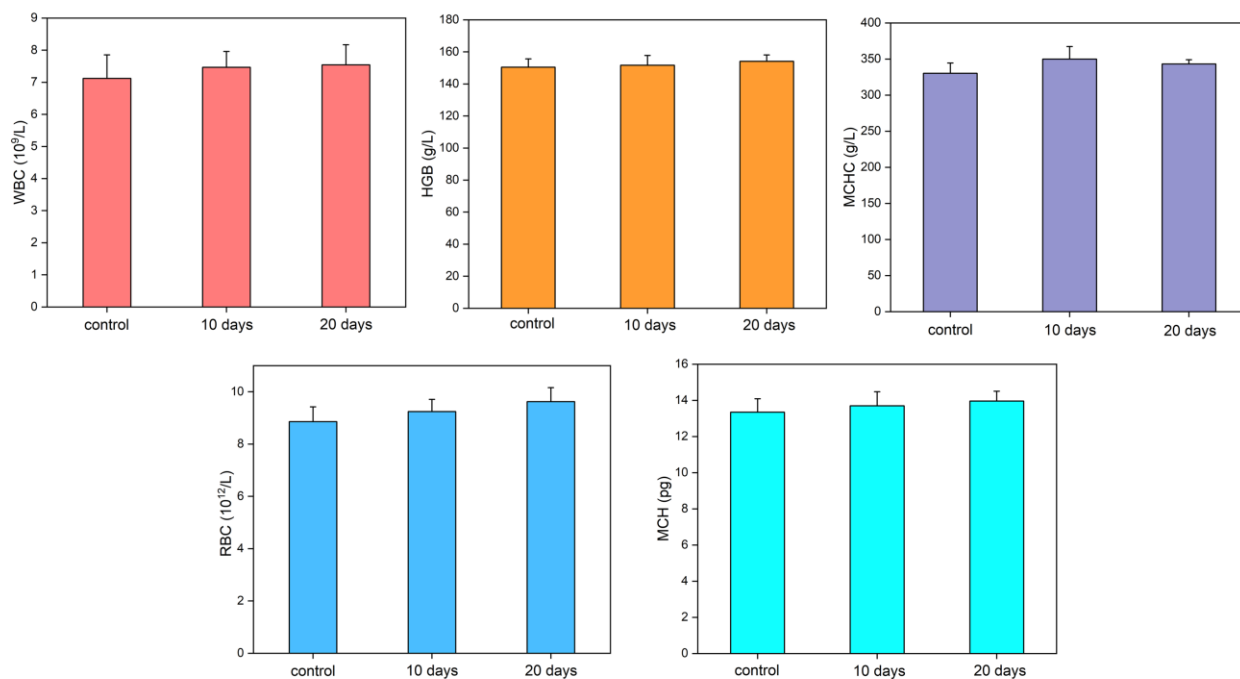


**Figure S18.** Hematology assays of healthy mice at day 10 and 20 after intravenous injection of the probe. The hematological biomarkers of white blood cells (WBC), hemoglobin (HGB), mean corpuscular hemoglobin (MCH), red blood cells (RBC) and mean corpuscular hemoglobin concentrations (MCHC) of the experimental group was not significantly different from those of the control group. The control group was healthy mice that were treated with 0.9 % saline. Error bars represented the standard deviation of five mice.

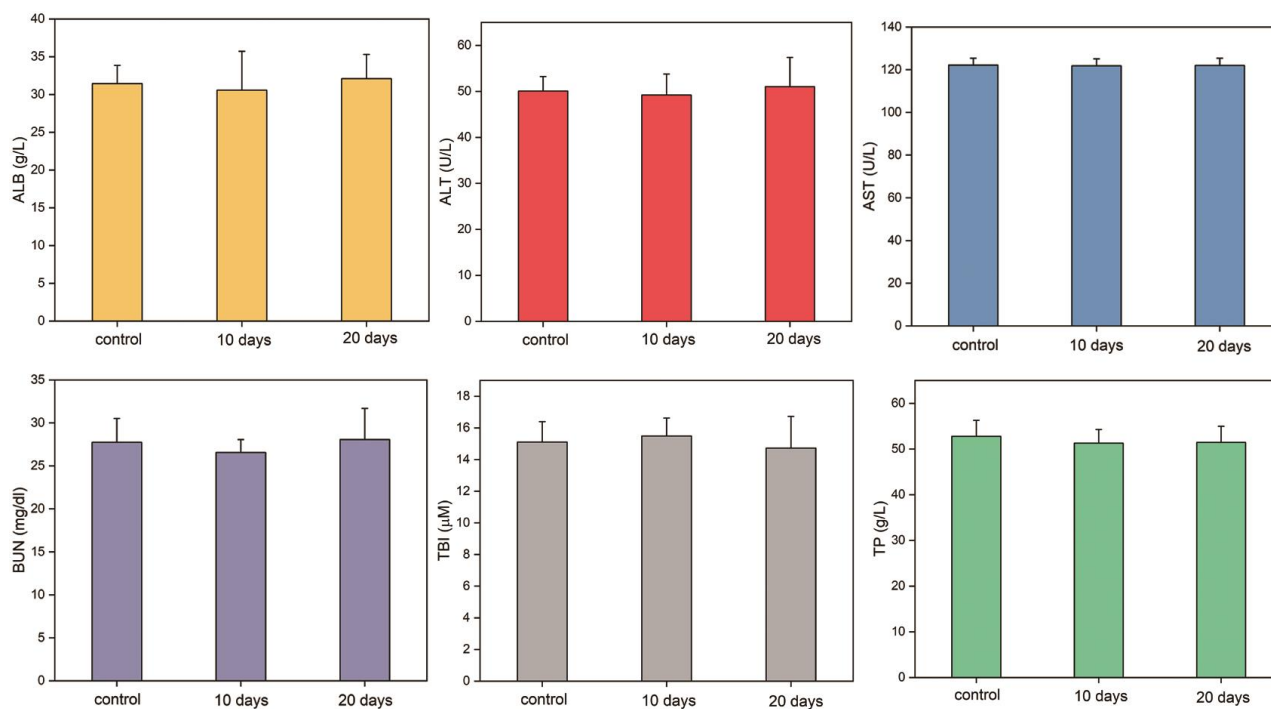


**Figure S19.** Biochemical blood analysis of healthy mice at day 10 and 20 after intravenous injection of the probe. The control group was healthy mice that were treated with 0.9 % saline. The organ function biomarkers of ALB, ALT, AST, BUN, TBL and TP exhibited no observable abnormality after treatment of the probe compared to those of the control group, indicative of negligible side effects of the probe. ALB: albumin; ALT: alanine aminotransferase; AST: aspartate aminotransferase;

BUN: blood urea nitrogen; TBL: total bilirubin; TP: total protein. Error bars represented the standard deviation of five mice.

**Table S1.** DNA sequences in this work.

<b>Name</b>	<b>Sequence (5'-3')</b>
A-strand <sup>a</sup>	NH <sub>2</sub> -C6-TTTTTAACCCCTAACCCCTAACTCTGCTCGACGGATTTT TTGGTGGTGGTGGTGTGGTGGTGGTGG
BHQ1-strand	AGGGTTAGGGTTTTT-BHQ1
Telomerase primer (TP)	AATCCGTCGAGCAGAGTT
Telomerase primer elongation product	AATCCGTCGAGCAGAGTTAGGGTTAGGGTT
Cy3-labeled strand	AGGGTTAGGGTTTTT-Cy3

<sup>a</sup>The green region represents the sequence of AS1411 aptamer; the blue region shows the complementary part of telomerase primer; the red region indicates the complementary part of BHQ1-ended DNA or Cy3-ended DNA.